

# Photoacoustic Spectroscopy, Theory

András Miklós, Stefan Schäfer and Peter Hess,  
University of Heidelberg, Germany

Copyright © 1999 Academic Press

**ELECTRONIC SPECTROSCOPY/  
VIBRATIONAL, ROTATIONAL &  
RAMAN SPECTROSCOPIES**

**Theory**

## Introduction

The phenomenon of the generation of sound when a material is illuminated with nonstationary (modulated or pulsed) light is called the photoacoustic (PA) effect. Photoacoustic spectroscopy (PAS) is the application of the PA effect for spectroscopic purposes. It differs from conventional optical techniques mainly in that, even though the incident energy is in the form of photons, the interaction of these photons with the material under investigation is studied not through subsequent detection and analysis of photons after interaction (transmitted, reflected or scattered), but rather through a direct measurement of the effects of the energy absorbed by the material. Since photoacoustics measures the transient internal heating of the sample, it is clearly a form of calorimetry as well as a form of optical spectroscopy.

In the following discussion the complex PA effect will be divided into three steps:

Heat release in the sample material due to optical absorption.

Acoustic and thermal wave generation in the sample material.

Determination of the PA signal in a PA detector.

A quantitative analysis of the PA signal is possible only when all three steps can be described quantitatively. Up to now this could be achieved only in a few special cases. Excitation of rovibrational levels leads to a complete transformation of the absorbed radiation into heat, whereas for vibronic excitation competing channels exist such as emission of radiation and photoinduced reactions. In this latter case, additional information on these competing channels is needed for the theoretical description.

A quantitative treatment of acoustic and thermal wave generation is usually possible only for simple excitation geometries, as can be realized by laser excitation, using the basic equations of fluid mechanics and thermodynamics.

The PA signal finally detected with a calibrated microphone for quantitative analysis is also influenced by the shape and nature of the photoacoustic cell, which impose boundary conditions on the evolution of the generated acoustic waves. However,

only for highly symmetric resonant setups with high  $Q$  factors does a theoretical analysis seem to be possible. This means that for most experimental arrangements used in PAS a quantitative signal analysis cannot be achieved and more or less drastic approximations have to be introduced into the signal analysis.

## Heat release in the sample material due to optical absorption

The interaction of photons with the material may produce a series of effects (Figure 1). If any of the incident photons are absorbed by the material, internal energy levels (rotational, vibrational, electronic) within the sample are excited. The excited state may lose its energy by radiation processes, such as spontaneous or stimulated emission, and by nonradiative

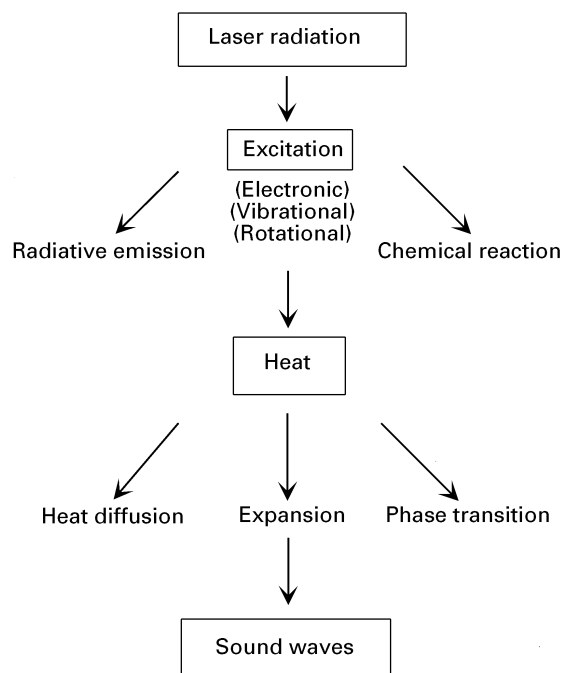


**Figure 1** Elementary processes occurring during PA signal generation. The absorbed photon energy is partly transformed into heat and acoustic energy.

deactivation, which channels at least part of the absorbed energy into heat. In a gas this energy appears as kinetic energy of the gas molecules, while in a solid it appears as vibrational energy of ions or atoms (phonons). In the case of vibrational excitation of gas molecules, radiative emission and chemical reactions do not play an important role, because the radiative lifetime of vibrational levels is long compared with the time needed for collisional deactivation at ordinary pressures and the photon energy is too small to induce reactions. Thus the total absorbed energy is released as heat. However, in the case of electronic excitation, the emission of radiation and chemical reaction processes may compete efficiently with collisional deactivation. Chemical reactions may also contribute to the release of heat, and thus they may increase the PA effect. If photodissociation occurs, for example, the local increase of the number of molecules and the thermalization of the recoil energy of the fragments generates a local pressure and temperature rise.

The heat release due to optical absorption in the sample material can be modelled by a rate equation. If it is assumed that the thermalization of the absorbed photon energy can be described by a simple linear relaxation process, the heat released per unit volume and time can be determined by solving the rate equation. If the near-resonant vibration–vibration (V-V) and the vibration–translation (V-T) relaxation are the fastest processes (as, for example, in many gases at atmospheric pressure), the heat power density will be proportional to the absorption coefficient and to the incident light intensity. In cases of very short laser pulses or high light intensity, optical saturation may occur. Then the heat production will be a nonlinear function of the light intensity and absorption coefficient. The timescales of the temporal evolution of the processes involved are summarized in Figure 2. The heat release may be delayed in gas mixtures if the excess energy of the excited molecule can be channelled by collisions to a long-lifetime transition of another species.

### Acoustic and thermal wave generation in the sample material

Sound and thermal wave generation can be theoretically described by classical disciplines of physics such as fluid mechanics and thermodynamics. The governing physical laws are the energy, momentum and mass conservation laws, given in the form of the heat-diffusion, Navier–Stokes and continuity equations, respectively. The physical quantities characterizing the PA and photothermal (PT) processes are the temperature  $T$ , pressure  $P$  (mechanical stress in case of

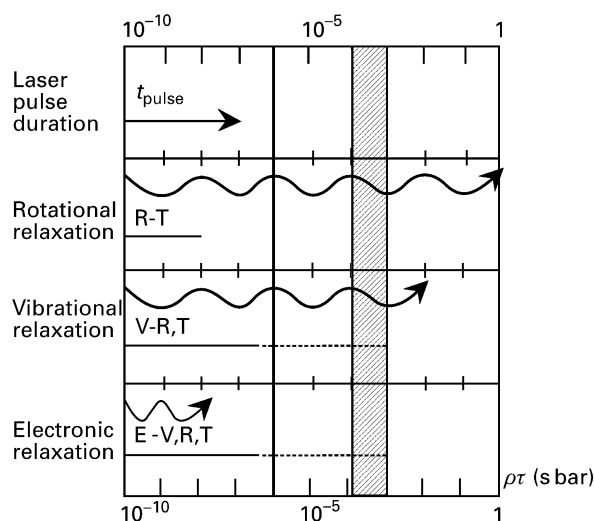


**Figure 2** Timescales for the radiative emission and relaxation processes. The shaded area indicates the typical response time of a PA resonator equipped with a microphone. The thick line represents the acoustic transit time. The wavy lines depict the radiative emission and the horizontal lines the range of relaxation processes characterized by the relaxation time  $\tau$ .

solids), density  $\rho$  and three components of the particle velocity vector  $\mathbf{v}$ . As five equations are not enough to determine the above six quantities, a sixth equation is added, the thermodynamic equation of state in the form of  $\rho = \rho(P, T)$ . As the changes of  $\rho$ ,  $P$  and  $T$  induced by light absorption are usually very small compared to their equilibrium values, the equations can be linearized by introducing the deviations from the equilibrium values as new variables, by neglecting the products of the small variables and by regarding the equilibrium values as constants. Moreover, the velocity vector  $\mathbf{v}$  can always be separated into two components  $\mathbf{u}$  and  $\mathbf{w}$ , where  $\text{curl } \mathbf{u} = 0$  and  $\text{div } \mathbf{w} = 0$ . As the heat-diffusion and continuity equations are coupled only by the nonrotational component  $\mathbf{u}$  to the Navier–Stokes equation, the  $\mathbf{w}$  component of the particle velocity can be omitted. The governing equations may be written then as follows:

$$\frac{\partial \theta}{\partial t} + \frac{\gamma - 1}{\beta} \text{div } \mathbf{u} - \kappa_V \nabla^2 \theta = \frac{H(\mathbf{r}, t)}{\rho C_V} \quad [1]$$

$$\frac{\partial}{\partial t} \left( p - \frac{\beta}{K_T} \theta \right) + \frac{\text{div } \mathbf{u}}{K_T} = 0 \quad [2]$$

$$\rho \frac{\partial \mathbf{u}}{\partial t} + \text{grad } p - \frac{4\eta}{3} \nabla^2 \mathbf{u} = 0 \quad [3]$$

where  $\theta = T - T_0$ ,  $p = P - P_0$ ,  $\gamma$ ,  $\beta$ ,  $\kappa_V$ ,  $C_V$ ,  $H$ ,  $K_T$  and  $\eta$  are the new temperature and pressure variables, the

adiabatic coefficient, the heat expansion coefficient, the thermal diffusivity and heat capacity at constant volume, the density of the deposited heat power, the isothermal compressibility and the dynamic viscosity, respectively. For solid materials the Navier–Stokes equation is replaced by the wave equation of the longitudinal elastic waves.

The heat power density  $H$ , released in the material as the result of all nonradiative de-excitation processes, appears as the source term on the right hand side of the heat-diffusion equation. The spatial size and shape of the source volume depend on the light-beam geometry and on the absorption length in the material. Similarly, the time dependence of the heat source is determined by the time evolution of the light excitation and by the relaxation processes in the material. A photoacoustic effect can be generated by modulated radiation as well as by pulsed radiation. As the theoretical treatments of the two cases are different, they will be discussed separately.

### Modulated PAS

In this case the intensity (or the wavelength) of the incident light beam is modulated by an angular frequency  $\omega$  to generate the acoustic signal. As the modulation frequency is usually in the audio frequency range, the time delay between heat release and light intensity may be negligible. In this case the source term has the same time dependence as the light intensity. Assuming an  $\exp(i(\omega t - \mathbf{k}r))$  dependence of the variables,  $\theta$ ,  $p$  and  $\mathbf{u}$ , two independent plane wave solutions of Equations [1] and [3] can be derived: a thermal wave and a sound wave. The wave-lengths of the two plane waves can be determined from the corresponding eigenvalues of the wave vector  $\mathbf{k}$ , taking into account that the length  $|\mathbf{k}| = k$  of the wave vector (called wavenumber) is inversely proportional to the wavelength  $\lambda$  ( $k = 2\pi/\lambda$ ). The eigenvalues of the wavenumber for the thermal and sound wave may be given as  $k_{\text{th}}^2 \equiv -i\omega/\kappa_p$  and  $k_s^2 \equiv \omega^2/c^2(1 - i\omega\nu/c^2)$ , respectively, where  $\kappa_p$ ,  $\nu = 4\eta/3\rho$  and  $c$  are thermal diffusivity at constant pressure, the effective kinematic viscosity and the sound velocity, respectively. As the orders of magnitude of  $\kappa_p$  and  $c$  are  $10^{-5}$ – $10^{-7}$   $\text{m}^2 \text{ s}^{-1}$  and  $10^2$ – $10^4$   $\text{m s}^{-1}$  respectively, the wavelength of the thermal wave is much shorter than that of the sound wave. That is, two types of waves are simultaneously generated: a very strongly damped thermal wave with submillimetre wavelength, and a slightly damped sound wave with wavelengths in the centimetre to metre range. The thermal wave corresponds more or less to an isobaric thermal expansion, i.e. the changes of the temperature and density are much larger than that of the pressure. Because of the large damping coefficient,

this wave cannot propagate far away from the heated region; it appears only in the neighbourhood of the exciting light beam. In the sound wave a quasi-adiabatic state change propagates with the velocity of sound; here the orders of magnitude of the relative changes in pressure, temperature and density are the same. The amplitude of the periodic pressure change is proportional to the time-varying (AC) component of the released heat power density and inversely proportional to the modulation frequency.

As the average of the intensity of a modulated light beam is nonzero, the heat energy in the illuminated volume will rise continuously. Therefore, the temperature will slowly increase and the density will decrease until the heat deposition rate is equal to the loss rate due to heat conduction. This process is also governed by the heat-diffusion equation. For a closed cell the average density is constant; therefore a pressure rise will occur. This DC component of the released heat power density changes the thermodynamic state of the material, in particular in very small PA detectors ( $\approx \text{cm}^3$ ).

The amplitude of the periodic temperature change ( $\theta$ ) is also proportional to the AC component of the heat power density and inversely proportional to the modulation frequency. This means that the PA and PT effects are inherently coupled; the heat deposited by the interaction of radiation with the material generates a localized temperature rise, a thermal wave and a propagating sound wave. The first two effects will result in a periodically pulsating temperature distribution.

### Pulsed PAS

In the case of pulsed excitation, the absorption of photons ceases when the laser pulse is over, but the relaxation processes will continue until the full thermalization of the absorbed energy is achieved. Therefore, the duration of the thermal pulse is always longer than that of the light pulse. Nevertheless, the heat pulse may be regarded as instantaneous acoustic excitation if the characteristic time of the acoustic event is much larger than the duration of the heat pulse. Two quantities characterize the acoustic process, namely the transit time  $\tau_s$  of the sound through the heated volume and the response time of the PA detector. The value of  $\tau_s$  is usually in the microsecond range (Figure 2), because the laser beam diameter usually does not exceed a few millimetres in PAS. The PA response time depends on the period of the eigenmodes of the detector and is usually in the millisecond range (Figure 2). As the pulse duration of most pulsed lasers is in the nanosecond range, and in many cases, such as V-V and V-T

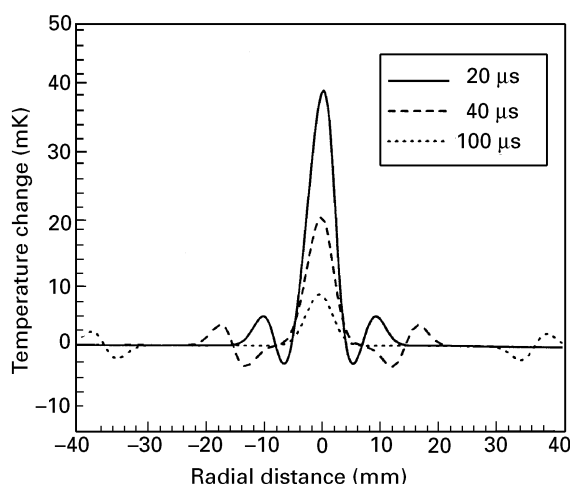


**Figure 3** Modelling of the gas temperature distribution as a function of the radial distance from the light excitation source. The diameter of the light beam was 6 mm and the pulse duration 20 ns. The three curves represent three different time delays after illumination.

relaxation in gases, the relaxation time is also in the nanosecond to microsecond range, the source term of Equation [1] may be regarded as a Dirac-delta pulse. The governing equations (Eqns [1] to [3]) can be solved by the Green's function technique, taking into account the Green's functions of both the thermal and acoustic problems. The solution is composed of a slowly broadening quasi-Gaussian temperature distribution and an outward propagating sound pulse of duration  $\geq 2\tau_s$ . After a short time the sound pulse will be separated from the thermal distribution, allowing the measurement of both features separately (Figure 3). The spatial symmetry of the solution depends on the shape and size of the heated region. In strong absorbers, the heated region is usually small compared to the sound wavelength; therefore mostly spherical sound waves are produced. In weakly absorbing gases, cylindrical acoustic waves are generated. The outward-propagating primary wavefront can be detected by appropriate high-frequency pressure sensors. As the achievable sensitivity and signal-to-noise (S/N) ratio are small, the direct detection of the primary waves has no practical significance. In practice the acoustic excitation takes place inside a PA detector, and the time evolution of the acoustic signal is strongly influenced by the properties of this detector.

### Determination of the PA signal in a PA detector

The actual solutions of the governing equations (Eqns [1] to [3]) depend on the boundary conditions

determined by the type and geometry of the PA detector. In gas-phase photoacoustics, the PA detector consists of a cavity and a microphone to monitor the acoustic signal. From an acoustic point of view, the PA detector is a linear acoustic system that responds in a characteristic way to an excitation. The acoustic properties of the PA detector can be determined independently using acoustic modelling techniques or by measuring them in an acoustic laboratory. Once the acoustic properties are known, the response of the PA detector for any kind of PA excitation can be determined by calculation. Although PA detectors can usually be used with both modulated and pulsed excitation, the theoretical description of the two cases will be presented separately.

### PA detectors excited by modulated light

A simple PA detector consists of a cavity and a microphone to monitor the acoustic signal (Figure 4A). Even such a simple system has acoustic resonances. If the modulation frequency is much smaller than the lowest resonance, the PA detector or PA cell operates in a nonresonant mode. Such a PA cell is frequently called a 'nonresonant' cell in the literature. In this case the sound wavelength is much larger than the cell dimensions and thus the sound cannot propagate. The average pressure in the detector will oscillate with the modulation frequency. The amplitude of the oscillation may be determined by integrating Equations [1] to [3] over the volume of the detector. The pressure amplitude will be inversely proportional to the volume of the cell. The photoacoustically generated pressure can be approximated by the expression

$$p(\omega) = \frac{(\gamma - 1)\alpha l W_L}{i\omega V_{\text{cell}}} \quad [4]$$

where  $\alpha$ ,  $l$ ,  $W_L$ ,  $\omega$ ,  $V_{\text{cell}}$  and  $\gamma$  denote the absorption coefficient of the material at the light pass length, the incident light power, the modulation frequency, the cell volume and the adiabatic coefficient of the material, respectively. In the case of a small cell and low modulation frequency, the signal may be quite large. The PA signal has a  $90^\circ$  phase lag with respect to the light intensity. Unfortunately, the noise also increases with decreasing frequency and volume; thus the S/N ratio will usually decrease.

As mentioned, the acoustic and thermal processes are inherently coupled. Until the cell dimensions are much larger than the size of the pulsating thermal distribution, the simple model described above can be applied. The thermal wave is usually not completely

damped at the walls of the cell in the case of a very small cell and very low modulation frequency. Then both the average temperature and the amplitude of the temperature oscillation will be influenced by the heat conduction through the cell walls to the environment. As in a closed cell the pressure is proportional to the temperature, the PA signal will also depend on the heat conduction through the walls. Since the theoretical modelling of this effect is practically impossible, such small cells and very low modulation frequencies allow only a qualitative signal analysis.

A special case should be mentioned here, one of the oldest arrangements among PA detectors. Termed the ‘gas-microphone cell’ it is used for investigating samples of condensed materials (Figure 4B). It usually consists of a small cylinder equipped with a sample holder, a microphone and a window. The gas in the cell is nonabsorbing; only the sample and the backing material (in the case of an optically thin sample) absorb the incident radiation. The PA signal is produced in an indirect way; the thermal waves generated in the solid sample are transmitted to the gas, and the periodic heat expansion of the gas above the sample surface acts as a piston and produces pressure oscillations in the closed cell volume. As the penetration depth of the thermal wave is usually much smaller than the diameter of the light beam, one-dimensional theoretical modelling is possible.

In resonant photacoustics, an acoustic resonator with an optimized geometry such as a cylinder or sphere is used as the gas cell. Such an acoustic system has several eigenresonances, whose frequencies depend on the geometry and size of the cavity. For a lossless cylinder, the resonance frequencies of the different eigenmodes can be calculated from the equation

$$f_{n,m,n_z} = \frac{c}{2} \sqrt{\left(\frac{\chi_{m,n}}{R}\right)^2 + \left(\frac{n_z}{L}\right)^2} \quad [5]$$

where  $c$ ,  $R$  and  $L$  are the sound velocity of the gas in the cavity, the radius and the length of the cylinder, respectively. The indices  $m$ ,  $n$  and  $n_z$  may take the values 0, 1, 2, etc. The quantity  $\chi_{m,n}$  is the  $n$ th zero of the derivative of the  $m$ th-order Bessel function divided by  $\pi$ .

When only one index is nonzero, the eigenmodes separate into longitudinal ( $n_z \neq 0$ ), radial ( $n \neq 0$ ) and azimuthal ( $m \neq 0$ ) modes (Figure 5). In the other mixed eigenmodes the spatial distribution of the sound pressure is much more complicated.

The modulation frequency may be tuned to one of the eigenresonances of the PA detector. Such ‘resonant PA cells’ or detectors have found widespread application in PA trace gas measurements. Since the eigenmodes of a lossless cavity are orthogonal, the sound pressure field in a lossy cavity can be approximated in the form of a series expansion of the eigenmodes, where the amplitudes of the terms depend on frequency. In fact, each amplitude function is a resonance curve characterized by the corresponding resonance frequency and quality factor ( $Q$  factor). The first term of the series expansion determines the sound pressure below the lowest resonance. To aid understanding of the behaviour of a resonant PA cell a computer simulation is shown in Figure 6, for which the frequency dependence of the PA signal at one end of a closed cylinder filled with a strongly absorbing gas was calculated. It can be seen that several resonances (the odd-numbered longitudinal ones) lie on a nonresonant curve. For well-separated sharp resonances, only two terms of the series expansion are necessary to determine the sound pressure around a certain resonance. These are the first nonresonant term, which is independent of the spatial coordinates but depends inversely on the frequency, and the resonant term, corresponding to the selected eigenmode. This term depends on the overlap of the acoustic mode pattern and the light beam distribution, on the position of the microphone and on the

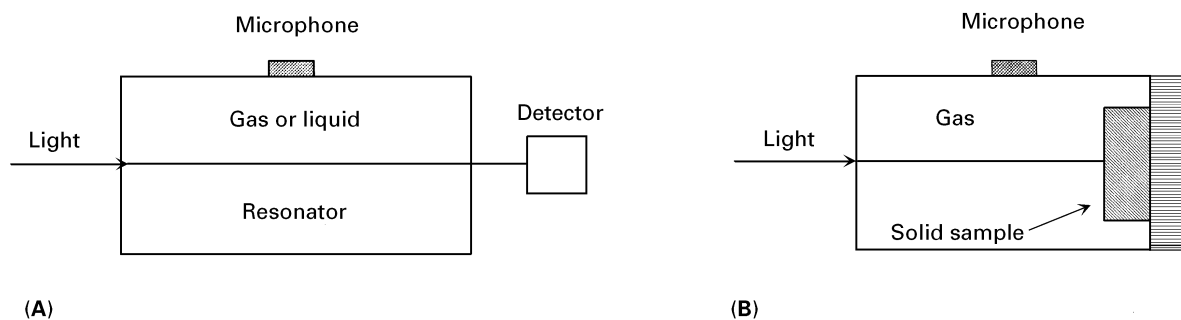


**Figure 4** PA setups for monitoring the PA signal with a microphone in a resonator: (A) gas or liquid, (B) solid sample in a gas microphone cell.

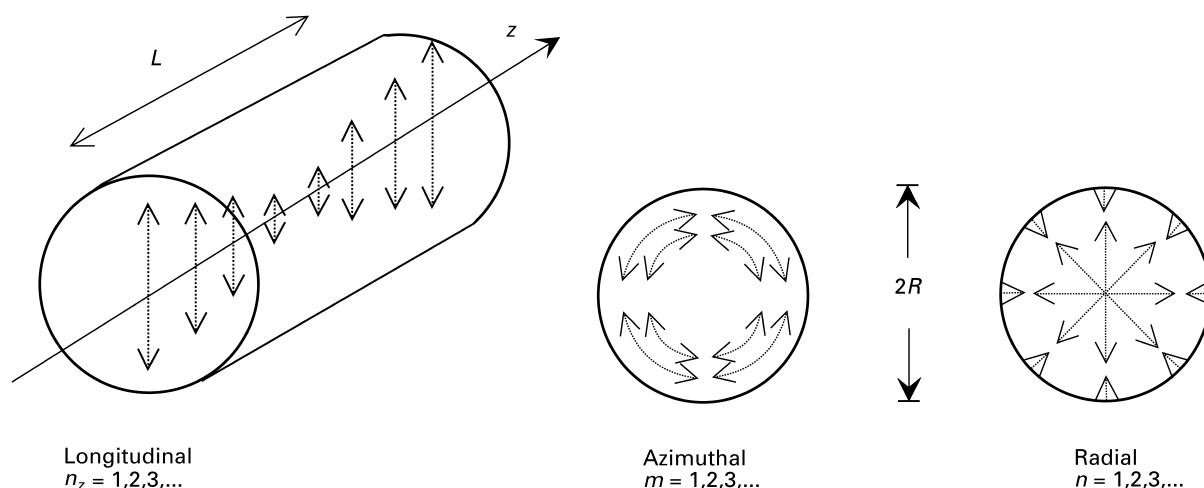


**Figure 5** Schematic representation of the longitudinal, azimuthal and radial acoustic modes in a cylindrical resonator.

quality factor of the eigenresonance. In the case of high  $Q$  factors ( $Q > 100$ ), the contribution of the nonresonant term can be neglected and the PA signal amplitude at the resonance frequency  $\omega_j$  and at the position  $\mathbf{r}_M$  of the microphone can be calculated as

$$p(\mathbf{r}_M, \omega_j) = \frac{(\gamma - 1) l U_j p_j(\mathbf{r}_M) Q_j}{V_{\text{cell}} \omega_j D_j} \alpha W_L \quad [6]$$

where  $l$ ,  $p_j$ ,  $U_j$ ,  $Q_j$ ,  $D_j$ ,  $V_{\text{cell}}$ ,  $\alpha$  and  $W_L$  are the length of the light path within the cell, the pressure distribution of the  $j$ th eigenmode of the cell, the overlap integral of the light intensity distribution with  $p_j$ , the  $Q$  factor and the normalization factor of the  $j$ th eigenmode, the cell volume, the absorption coefficient and the incident light power, respectively. As the quantities in the first term of Equation [6] are independent of the light power and the absorption coefficient, the first term may be regarded as a characteristic setup quantity, called the ‘cell constant’, of the PA arrangement.

Since the resonance frequency depends on the speed of sound, a temperature drift of the gas inside the cavity causes a shift of all resonance frequencies. In modulated PAS this problem can be solved by temperature stabilization, by continuous monitoring of the gas temperature or by synchronizing the modulation frequency to the resonance peak using appropriate electronics.

As the modulation frequency of a CW light source may be arbitrary, a given PA detector can operate in both the nonresonant and resonant modes. The main advantage of resonant operation is the amplification of the PA signal by the  $Q$  factor of the resonator if the modulation frequency of the incoming light is

properly tuned to the selected acoustic resonance (‘acoustic amplifier’).

If the modulation frequency is so low that the corresponding wavelength is much longer than the dimensions of the detector, Equation [3] may be used to calculate the PA signal. Nonresonant operation is also possible by tuning the modulation frequency away from a resonance. In such cases the PA signal can be estimated by substituting  $Q = 1$  into Equation [6], but a better accuracy may be achieved by taking into account the nonresonant term and at least the neighbouring eigenmodes in the series expansion.

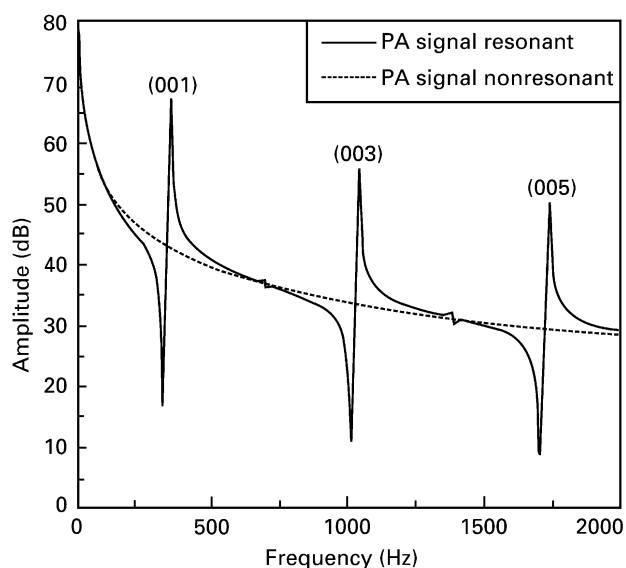


**Figure 6** Modelling of the frequency-dependent PA signal. The excited modes are the first (001), third (003) and fifth (005) longitudinal modes of the cavity. The dotted line shows the nonresonant contribution.

### PA detectors excited by light pulses

The absorption of a light pulse generates a primary acoustic pulse inside the PA detector. This pulse acts as a broadband acoustic source for the PA detector, exciting all eigenmodes simultaneously. If the acoustic transit time is much shorter than the period of the detected eigenmode of the resonator, the excitation of the PA signal can be regarded as instantaneous (Figure 2). In this case the slow PA detector responds to the excitation similarly to the way in which a ballistic pendulum or galvanometer responds to force or charge pulses; a sudden rise of the PA signal followed by a slow decay can be observed. The amplitude of the first period of the sound pressure oscillation will be proportional to the released heat energy. Thus, a pulsed PA detector can be used for absolute (calorimetric) measurement of that part of the absorbed light energy that was converted to heat. As calibrated microphones are available, the absolute measurement of the photoacoustically generated sound pressure is possible. The solutions of Equations [1] to [3] can again be given in the form of a series expansion of the orthogonal eigenmodes, but in this case the amplitudes will depend not only on the frequency but also on time. A PA cell for pulsed operation is designed for optimal excitation of a selected eigenmode. This mode should be well separated from the neighbouring ones and should have a high  $Q$  factor. As the PA response in the time domain shows a very complicated behaviour, it is much better to evaluate the PA signal by converting the time signal to the frequency domain using Fourier transformation. A part of the frequency spectrum measured in a cylindrical cell, optimized for the first radial mode, is shown in Figure 7. The PA signal amplitude at the peak of the selected resonance can be determined from the theory as

$$p(r_M) = \frac{(\gamma - 1) IU_j p(r_M)}{V_{\text{cell}} D_j} \alpha E_L \quad [7]$$

where  $E_L$  is the pulse energy. As the fast Fourier transform (FFT) algorithm applied for calculating the spectrum delivers the average spectrum of the signal over the recorded time window, the amplitude of the resonance peak has to be corrected in order to obtain the value of  $p(r_M)$ . The ratio of the corrected PA amplitude and laser pulse energy depends only on the product of several geometry factors and the absorption coefficient  $\alpha$  of the absorbing component. In contrast to Equation [6], the PA signal amplitude  $p(r_M)$  in Equation [7] does not depend on the  $Q$  factor of the cavity, which cannot be calculated

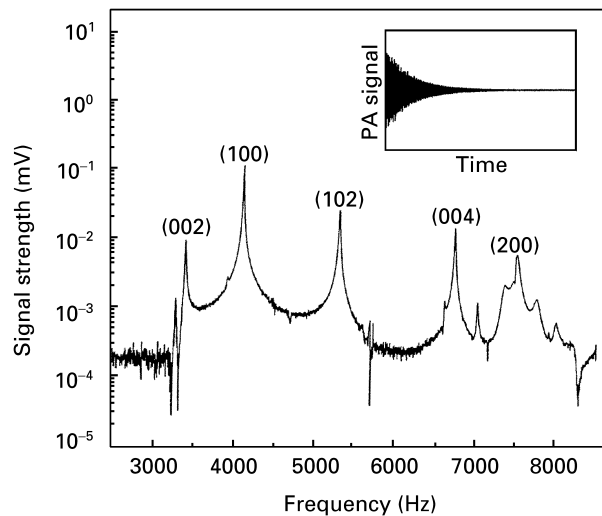


**Figure 7** Time-dependent PA signal recorded by a microphone (inset) and corresponding frequency spectrum of a cylindrical resonator. In the displayed frequency range, the second longitudinal (002), first radial (100), combination (102), fourth longitudinal (004) and second radial (200) modes of the resonator are detected.

with high accuracy theoretically. Thus, pulsed PAS is an absolute method for measuring the absorption coefficient. Since  $\alpha$  is given as the product of the number density  $N$  and the absorption cross section  $\sigma$  of the absorbing molecules, pulsed PAS can be applied for both spectroscopic studies (known  $N$ ) and trace gas analysis (known  $\sigma$ ).

### Summary

The theory of PAS is sufficiently complicated that only an overview could be presented. In the theoretical description of a given PAS experiment, a separated treatment of the three physical processes, as presented here, is often not possible. Moreover, important quantities of the theory, such as the  $Q$  factor and the overlap integral  $U_j$ , are very difficult to keep under control. Small changes in the experimental adjustment (e.g. microphone position or beam focusing) may cause considerable changes, so that the agreement between theory and experiment may be degraded. As the PA signal does not depend on the  $Q$  factor in pulsed PAS, and the  $Q$  factor, which is needed only for calculating the correction factor, can be derived from the measured spectrum, pulsed PAS is more suitable for quantitative measurements than is modulated PAS. On the other hand, the probability of optical saturation is quite high in pulsed PAS, since the pulse energy of the available laser sources is usually in the millijoule range and the corresponding instantaneous power in the kilowatt to megawatt range. Therefore,

the linear dependence of the PA signal on the pulse energy must always be checked in pulsed PAS.

### List of symbols

$c$  = sound velocity;  $C_V$  = heat capacity at constant volume;  $D_j$  = normalization factor of  $j$ th eigenmode;  $E_L$  = pulse energy;  $H$  = heat power density;  $k = |\mathbf{k}|$ ;  $\mathbf{k}$  = wave vector;  $K_T$  = isothermal compressibility;  $L$  = cavity length;  $l$  = light path length;  $P$  = pressure;  $p = P - P_0$ ;  $Q_j = Q$  factor of  $j$ th eigenmode;  $\mathbf{r}$  = position vector;  $R$  = cavity radius;  $T$  = temperature;  $U$  = overlap integral;  $\mathbf{u}$ ,  $\mathbf{v}$  = particle velocity vector;  $W_L$  = incident light power;  $\alpha$  = absorption coefficient;  $\beta$  = thermal expansion coefficient;  $\gamma$  = adiabatic coefficient;  $\eta$  = dynamic viscosity;  $\theta = T - T_0$ ;  $\kappa_V$ ,  $\kappa_P$  = thermal diffusivity at constant volume, pressure;  $\lambda$  = wavelength;  $\nu$  = effective kinematic viscosity =  $4\eta/3\rho$ ;  $\rho$  = density;  $\tau_s$  = transit time of sound;  $\chi_{m,n}$  = the  $n$ th zero of the derivative of the  $m$ th-order Bessel function  $\times (1/\pi)$ ;  $\omega$  = angular frequency of modulation.

See also: **Laser Spectroscopy Theory; Light Sources and Optics; Photoacoustic Spectroscopy, Applications.**

### Further reading

Diebold GJ (1989) Application of the photoacoustic effect to studies of gas phase chemical kinetics. In: Hess P (ed)

*Photoacoustic, Photothermal and Photochemical Processes in Gases*, pp 125–170, Vol 46 in Topics in Current Physics. Berlin: Springer.

Fiedler M and Hess P (1989) Laser excitation of acoustic modes in cylindrical and spherical resonators: theory and applications. In: Hess P (ed) *Photoacoustic, Photothermal and Photochemical Processes in Gases*, pp 85–121, Vol 46 in Topics in Current Physics. Berlin: Springer.

Hess P (1992) Principles of photoacoustic and photothermal detection in gases. In: Mandelis A (ed) *Progress in Photothermal and Photoacoustic Science and Technology*, Vol 1, pp 153–204. New York: Elsevier.

Morse PM and Ingard KU (1986) *Theoretical Acoustics*. Princeton, NJ: Princeton University Press.

Pao YH (1977) *Optoacoustic Spectroscopy and Detection*. New York: Academic Press.

Rosencwaig A (1980) *Photoacoustics and Photoacoustic Spectroscopy*. New York: Wiley.

Schäfer S, Miklós A and Hess P (1997) Pulsed laser resonant photoacoustics/applications to trace gas analysis. In: Mandelis A and Hess P (eds) *Progress in Photothermal and Photoacoustic Science and Technology*, Vol 3, pp 254–289. Bellingham, WA: SPIE.

Schäfer S, Miklós A and Hess P (1997) Quantitative signal analysis in pulsed resonant photoacoustics. *Applied Optics* 36: 3202–3211.

West GA, Barrett JJ, Siebert DR and Reddy KV (1983) Photoacoustic spectroscopy. *Review of Scientific Instruments* 54: 797–817.

Zharov VP and Letokhov VS (1986) *Laser Optoacoustic Spectroscopy*. Berlin: Springer.

## Photoelectron Spectrometers

László Szepes and György Tarczay,  
Eötvös University, Budapest, Hungary

Copyright © 1999 Academic Press

HIGH ENERGY  
SPECTROSCOPY

Methods & Instrumentation

This article is centred on one of the most important molecular spectroscopic applications of photoionization. First, conventional photoelectron spectrometers based on the pioneering work of Turner, Vilesov and Siegbahn are reviewed, the basic building elements are shown and the principles of operation are discussed. Besides the conventional photoelectron experiment, threshold analysis and photoelectron-photoion coincidence spectroscopy as well as conceptually new techniques related to laser photoionization are discussed briefly.

### Conventional photoelectron spectrometers

Photoelectron spectroscopy is a molecular spectroscopic method which is based on photoionization. If an atom or molecule ( $M$ ) is irradiated with photons of larger energy than the ionization energy of the particle ionization may occur. The fundamental process and its energetics are given by the following equations:

